

Symmetry breaking in photon-induced Al $L_{2,3}VV$ Auger decays

T. Greber,* J. Osterwalder, S. Hüfner,[†] and L. Schlapbach
Institut de Physique, Université de Fribourg, 1700 Fribourg, Switzerland
 (Received 25 June 1991; revised manuscript received 30 September 1991)

The angular distributions of Si $K\alpha$ -excited Al $1s$ photoemission, the $L_{2,3}VV$ Auger line, and its 15-eV high-energy satellite (L^*VV), are measured over the hemisphere above the Al(001) surface, with an experimental geometry such that the incident radiation breaks the mirror symmetries associated with (100) and (110) crystal planes. Strong photon-polarization effects are seen in $1s$ photoemission, and are also reproduced by single-scattering calculations. A symmetry analysis indicates that in the high-energy satellite the photon-induced mirror-symmetry breaking persists. A comparison with single-scattering calculations shows that the $L_{2,3}VV$ and the L^*VV decays produce Auger electrons with different angular-momentum character.

Most angle-scanned Auger electron diffraction (AED) or photoelectron diffraction (PD) studies investigating the structure of surfaces^{1,2} have reported their results as a series of polar and/or azimuthal scans, i.e., one-dimensional cuts through the hemisphere above a surface. Only recently have two-dimensional 2π scans of the electron flux been published, in order to explore the full diffraction information.³⁻⁸ In this paper we would like to show how valuable such 2π intensity maps can be to recognize symmetries, and that in contrast to other claims⁵ most of the observed patterns can be well explained in terms of established diffraction theories.

At the kinetic energies below 200 eV considered in this study, multiple-scattering (MS) events must be present, even though simple single-scattering theories have been found to work surprisingly well.⁹ Moreover, the angular-momentum character of the outgoing electron wave prior to diffraction—the source wave—influences the observed diffraction pattern severely, and a careful analysis has to include transition matrix element effects.¹⁰ Only an isotropic emission of electrons from lattice sites is expected to reproduce the full symmetry of the surface under investigation.

In most cases PD and AED experiments are performed with a fixed orientation of x-ray incidence and electron emission directions while the crystal is rotated. In geometries with an oblique x-ray incidence the rotational symmetry will be reflected in the measurements, but anisotropic emission breaks the mirror-plane symmetries. Specifically, the electron emission is expected to be non-isotropic for all photoelectrons as well as for all Auger electrons which do not form a pure s wave or where the initial ion does not have a total angular momentum of $J = \frac{1}{2}$.¹¹ This latter statement is based, however, on the assumption that the symmetry of the atom is not affected by the ionization process.

The Si $K\alpha$ -excited $L_{2,3}VV$ spectrum of Al has a pronounced satellite with 15 eV higher kinetic energy than the main line. This satellite, here labeled as L^*VV , gave rise to various interpretations, first as that of a plasmon gain satellite^{12,13} and later as a decay of a doubly ionized

p orbital in the Al L shell.¹⁴ From an elegant comparison of Mg $K\alpha$ and Al $K\alpha$ excitation, Fuggle concluded that the high-energy satellite in the similar case of magnesium is related to double ionization.¹⁵ The hole created by Mg $1s$ photoemission is filled most prominently by Auger KLL decays, leaving two p holes in the L shell. This is considered to be the initial state for the L^*VV decay. A Mg-Si twin x-ray source permitted us to perform the same experiment for Al.

The experiment was performed in a modified VG Mark II ESCALAB spectrometer at a base pressure below 8×10^{-9} Pa. A Si-Mg twin anode, shielded with a thin Al window, supplied nonmonochromatized $K\alpha$ radiation at 1740 and 1253.6 eV, respectively. In our spectrometer, an oblique photon incidence with respect to the plane defined by the surface normal and the direction of electron detection (see Fig. 1) gives rise to the above-mentioned breaking of mirror symmetries. By rotation of the crystal, 3500 single data points (integrated intensities after a linear background subtraction) have been recorded over the hemisphere above the surface. The mesh of data points $I(\theta, \phi)$ was scanned in a series of azimuthal (ϕ) scans, with steps of $\Delta\phi = \Delta\theta\theta_{\max}/\theta$ ($\Delta\theta = 2^\circ$, $\theta_{\max} = 76^\circ$) which provided an almost uniform sampling of solid angle. Our data-acquisition procedure for 2π scans is described elsewhere in more detail.^{7,16} The electron analyzer acceptance cone was limited to a full opening of less than 4° . The Al(001) sample was cleaned by argon-ion bombardment and subsequent annealing to 750 K. The contamination with carbon and oxygen was kept below 10% of a monolayer.

Figure 2 shows spectra of the three signals considered here. In Fig. 2(a) the Si $K\alpha$ and Mg $K\alpha$ spectra along [001] (normal emission) are displayed. The intensity ratios between the $L_{2,3}VV$ and L^*VV peaks are 3.1 and 10.5 for Si $K\alpha$ and Mg $K\alpha$ excitation, respectively. In normalizing the Mg $K\alpha$ -excited L^*VV peak with the intensity ratio of the $KL_{2,3}L_{2,3}$ Auger decays observed with Si $K\alpha$ and Mg $K\alpha$ excitation, we obtain 1.1 times the Si $K\alpha$ L^*VV intensity, if linear backgrounds are used (see zoom inset). Therefore, the relatively weak Mg $K\alpha$ L^*VV

signal is probably induced by bremsstrahlung. This is in close agreement with the findings of Fuggle¹⁵ for Mg and suggests that the L^*VV peak is related to a $(1s^1 2s^2 2p^6 v^n)KLL \rightarrow (1s^2 2s^2 2p^4 v^n)LVV \rightarrow (1s^2 2s^2 2p^5 v^{n-2})$ stripping ionization, where v stands for the valence electrons.

In Fig. 2(b) the Si $K\alpha$ spectra along the [001] and [105] directions are shown. While the LVV and the Al $1s$ intensities increase slightly in going from normal emission to [105], which is only 11.3° away, the L^*VV intensity decreases by 44%. This can be taken as a first indication for a different emission character of the L^*VV electrons as compared to those of the LVV electrons, since this crossover effect cannot be explained in the framework of our theoretical simulations by the 9% smaller wavelength of the L^*VV electrons. We also point out that the spectral shape of the LVV emission changes significantly, from a rather broad peak at [001] to a narrower peak at [105]. This may be related to the energy-dependent partial l occupancy in the valence band¹⁷ and thus be another indication of the importance of the angular-momentum character of the outgoing electron wave for the angular distribution after final-state diffraction.

Figure 3(a) shows the PD pattern of the Si $K\alpha$ -excited Al $1s$ level at a kinetic energy of 180 eV with respect to the Fermi level. The polarization of the incoming photons destroys the 4-mm symmetry of the Al(001) substrate. This is most clearly seen near the $\langle 112 \rangle$ directions between the most prominent $\langle 011 \rangle$ forward scattering peaks, where two local maxima appear to be rotated off the (111) planes. On the other hand, the LVV emission [Fig. 3(c)] has an almost perfect 4-mm symmetry, as would be expected from an isotropic emitter. This finding is consistent with a dominant s -like source wave proposed for atomic Al.¹⁸ A careful inspection of the L^*VV 2π scan [Fig. 3(b)] indicates that here the mirror symmetry is broken in a similar subtle way as in $1s$ photoemission. This finding implies that the source wave is not isotropic, i.e., that the initial Al $(1s^1 2s^2 2p^6 v^3)$ ion is not spherically symmetric and/or that the outgoing $1s$

photoelectron breaks the symmetry of the charge distribution in the following Auger process.

In order to quantitatively assess these symmetry arguments, we compare in Fig. 4 the mm mirror symmetry with the fourfold rotational symmetry as a function of the mirror-plane angle Φ with respect to the (100) crystal plane. We form the ratio $R(\Phi)$ of the sum of $[\sum(1 - I_{ji}/I_{jm})^2]^{1/2}$ of all 4 tuples I_{ji} in the experimental spectra which should be equivalent for the mm and the fourfold symmetry, respectively, where I_{jm} is the mean value of the tuple j . Due to the partial degeneracy of the mm symmetry (if a pair of intensities lies on a mirror plane), R has to be normalized to unity for an isotropic 2π scan. A value of $R=1$ and an even function $[R(\Phi)=R(-\Phi)]$ corresponds to a perfect 4-mm symmetry. From Fig. 4 it becomes clear that the mirror symmetry is closest to the fourfold symmetry for the (110) and (100) crystal planes as mirrors. The matching is not as perfect as we find it, e.g., for a Mg $K\alpha$ -excited Al $2s$

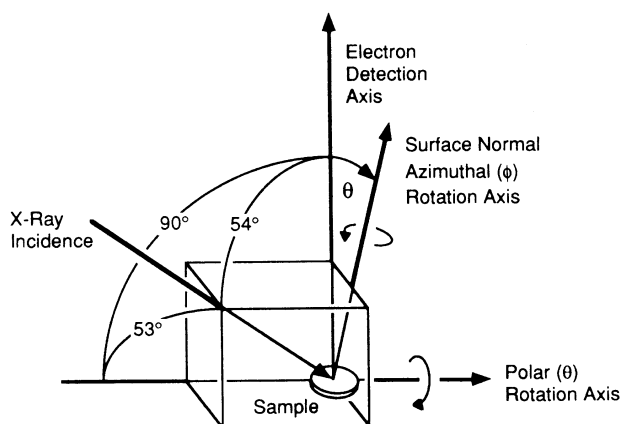


FIG. 1. Sampling geometry in our experiment. The oblique angle between the incoming photons and the plane defined by the azimuthal rotation axis (surface normal) and the direction to the detector induces for nonisotropic emitters a mirror-symmetry breaking.

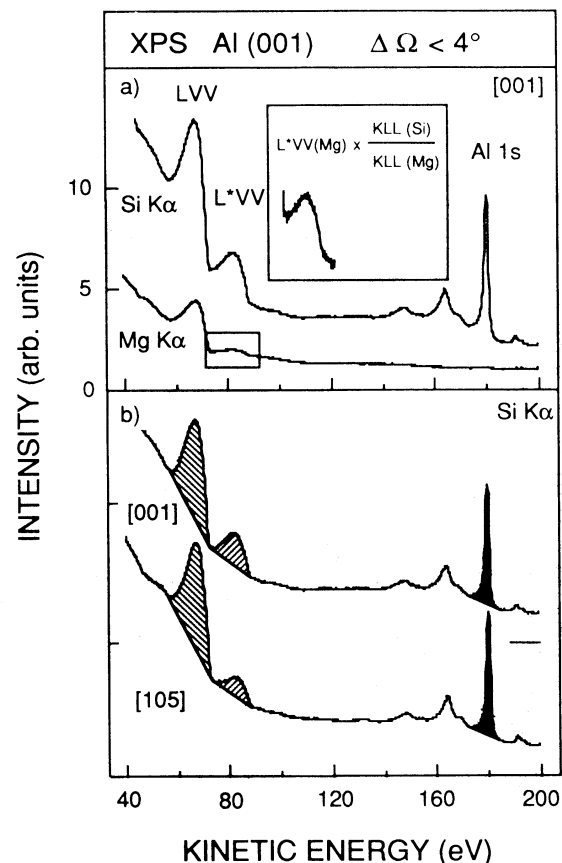


FIG. 2. Energy-resolved electron spectra from Al (001) between 200- and 40-eV kinetic energy with respect to the Fermi level. (a) Comparison of Mg $K\alpha$ - and Si $K\alpha$ -excited spectra. The Si $K\alpha$ spectrum exhibits Al $1s$ emission and the subsequent plasmon loss features. The LVV Auger line at 70 eV has a high-energy satellite (L^*VV) at 85 eV, the spectral weight of which depends crucially on the excitation source. The zoom inset shows, however, that the satellite scales with the intensity of the KLL Auger decay (not shown). (b) Si $K\alpha$ -excited spectra along the surface normal and along the [105] direction. The peak areas which are recorded in the 2π scans shown in Fig. 3 are shaded.

scan ($R_{\min}=0.9$, not shown). The most prominent deviation from the 4-mm symmetry is observed in the Al 1s scan ($R_{\min}=2.1$). While the deviation is small in the LVV scan ($R_{\min}=1.3$), it is still significant for L^*VV ($R_{\min}=1.8$). The minima in the Al 1s and the L^*VV scans appear to be shifted away from the angle where LVV shows a minimum. Since the spectral background may influence the signal we are extracting, the same symmetry analysis has been performed with the background intensities below the peaks (dotted lines). In the case of Al 1s and L^*VV the underlying background shows less symmetry breaking, indicating that this is indeed an effect in the signal. This suggests that the L^*VV electrons are not emitted from a spherically symmetric Al ($1s^1 2s^2 2p^6 v^3$) ion and/or that they have a memory of how their initial state was created. This would imply that the $2p$ shell configuration for the L^*VV decay is somehow polarized by the precedent 1s photoionization.

The LVV signal has a higher mm symmetry than its background [Fig. 4(c)]. Therefore, it is difficult to make a quantitative statement on the symmetry breaking in the LVV decay. Still, it was shown by Flügge, Mehlhorn, and Schmidt¹⁹ for the different case of Mg that $2p$ photoionization leads to anisotropic $L_{2,3}MM$ emission due to a

nonuniform occupation of magnetic sublevels in the hole state, and some degree of mirror-symmetry breaking may therefore be expected also in Al.

We simulated with our single-scattering cluster program^{1,20} [Figs. 3(d)–3(f)] the experimentally observed patterns [Figs. 3(a)–3(c)]. In the case of 1s photoemission, the emitter was described by two incoherent p waves along two orthogonal polarization vectors of the unpolarized x rays. This reproduces our experimental intensity map quite well, and particularly, the mirror-symmetry breaking [Figs. 3(a) and 3(d)]. Apparently, MS effects are highly damped due to a very short inelastic mean free path of the photoelectrons at this low energy.

To simulate Auger emission we adopted the model used by Aberdam *et al.*¹⁰ We summed the diffraction pattern over the $2l+1$ magnetic quantum numbers incoherently for a given source wave angular momentum l , effectively introducing isotropic emitters. In order to achieve a similar agreement between experiment and theory as obtained in the 1s photoemission, we expanded the basis set of emitted electrons to s -, p -, and d -wave intensities. This simple approximation does not include interference effects between the different partial waves, multiple scattering in the final state, valence-band in-

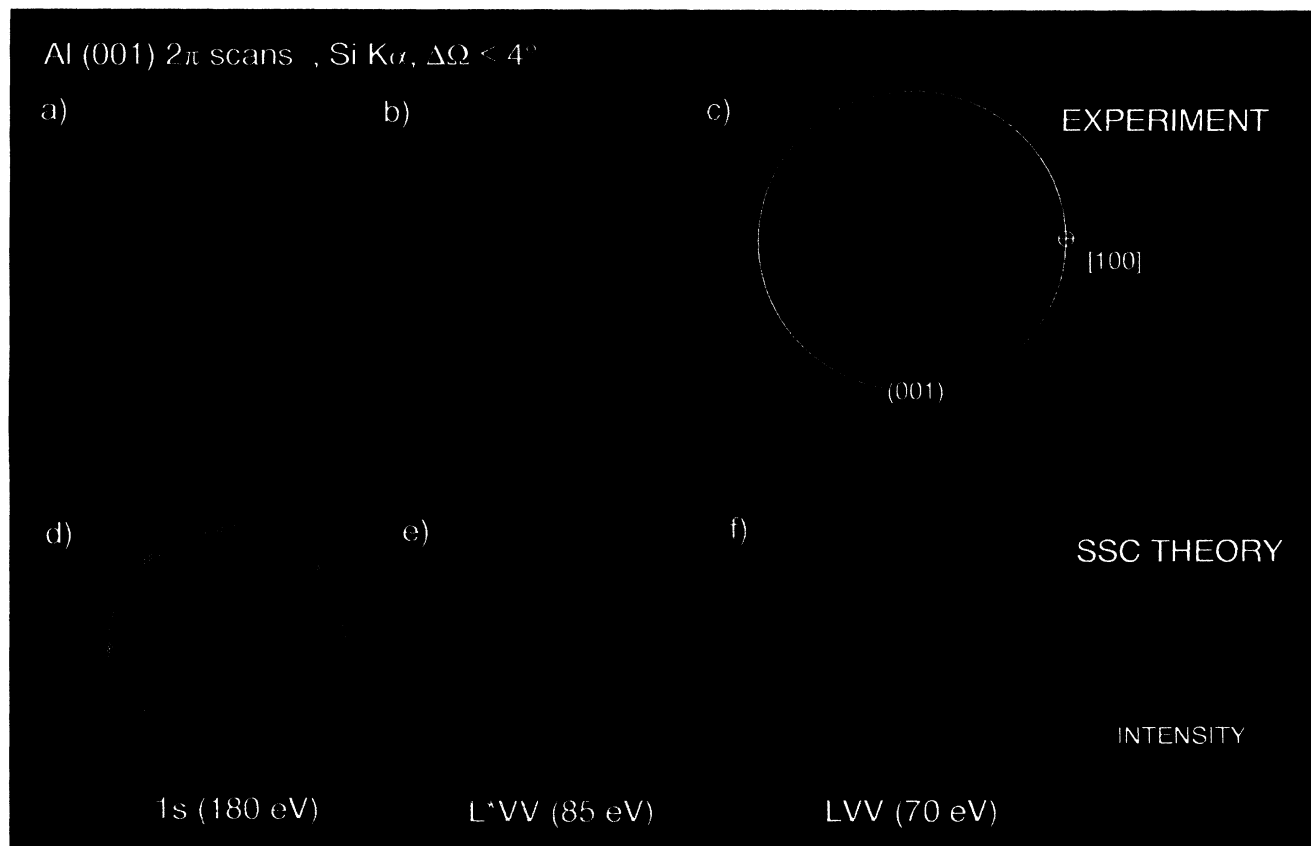


FIG. 3. Stereographically projected experimental and theoretical maps of electron emission intensities above an Al(001) surface. The intensities have been normalized with their maximum value in each plot. Each map consists of 3500 individually measured numbers. The experimental data [(a)–(c)] represent a total of 0.11, 0.22, and 0.21×10^9 counts for Al 1s (signal/background=0.27), L^*VV ($s/b=0.06$), and the LVV ($s/b=0.16$), respectively. The theory we applied to simulate these experiments considers single scattering only, and for the Al 1s emission p -wave final states aligned with the plane of polarization of our experiment. The L^*VV and LVV scans were simulated with incoherently added isotropic s , p , and d waves (see text).

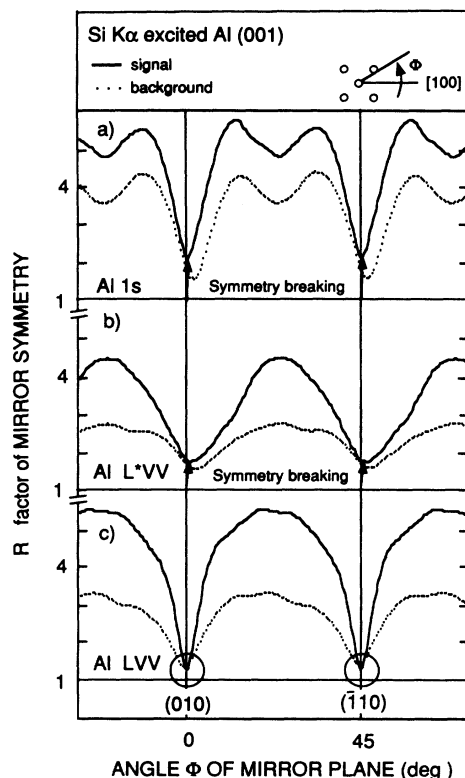


FIG. 4. Ratios between the mirror and fourfold symmetries for the Al $1s$, Al L^*VV , and the Al LVV 2π scans as a function of the angle of the mirror-plane azimuth. For details see the text.

duced anisotropies, and in particular it does not contain anisotropic source emission responsible for the measured mirror-symmetry breaking. However, it permits us to compare the least-squares-fit coefficients (s, p, d) for the two discussed Auger transitions. For LVV emission we

obtain values of (0.24, 0.26, 0.50) for the relative weights of s , p , and d emission, respectively. For L^*VV the values are (0.08, 0.67, 0.25). Although all simplifications mentioned above may influence the (s, p, d) weights to some degree, this simple analysis suggests that the outgoing LVV and L^*VV electrons have a different symmetry mixing. Furthermore, both decays do not exhibit a dominant $l=0$ character, as is expected from the single atoms.¹⁸ At this point we cannot decide to which extent this is caused by the band structure, the relaxation of the solid upon the core-hole creation, whether it results from a different screening in the much faster L^*VV process, or to which extent the second $2p$ hole plays the role of a spectator. It has to be noted that the LVV spectrum may be affected by a plasmon loss in the L^*VV transition and the LVV decay following an L^*VV decay. In the L^*VV decay the second $2p$ hole influences the angular-momentum character of the outgoing electrons. The strong ($Z+2$) excitation of the ground state might be responsible for an allowance of p - p -like $L_{2,3}VV$ decays which are expected to have a large p -wave matrix element as was pointed out for Si by Feibelman, McGurie, and Pandey.²¹ This is supported by the strong increase of the relative p weight in the L^*VV decay.

In conclusion, we have shown that the photoexcited Al $L_{2,3}VV$ Auger transition and its high-energy satellite L^*VV produce electron source waves with different angular-momentum character. A significant mirror-symmetry breaking is observed particularly in the angular distribution of the L^*VV , indicating a strong anisotropy of the associated source wave.

It is a pleasure to thank M. Erbudak in Zürich, W. Mehlhorn in Freiburg, and J. E. Hansen in Amsterdam for fruitful discussions. Financial support from the Schweizerischen Nationalfonds is gratefully acknowledged.

*Present address: Fritz-Haber-Institut der Max-Planck-Gesellschaft, Faradayweg 4-6, D-1000 Berlin 33, Germany.

†Permanent address: FB Physik, Universität des Saarlandes, D-6600 Saarbrücken, FRG.

¹C. S. Fadley, in *Synchrotron Radiation Research: Advances in Surface Science*, edited by R. Z. Bachrach (Plenum, New York, 1989).

²W. F. Egelhoff, Jr., *Crit. Rev. Solid State Mater. Sci.* **16**, 213 (1990).

³R. J. Baird, C. S. Fadley, and L. F. Wagner, *Phys. Rev. B* **15**, 666 (1977).

⁴H. Li and B. P. Tonner, *Phys. Rev. B* **37**, 3959 (1988).

⁵D. G. Frank, N. Battina, R. Golden, F. Lu, and A. T. Hubbard, *Science* **247**, 182 (1990).

⁶M. Seelmann-Eggebert and H. J. Richter, *J. Vac. Sci. Technol. B* **9**, 1861 (1991).

⁷J. Osterwalder, T. Greber, A. Stuck, and L. Schlapbach, *Phys. Rev. B* **44**, 13 764 (1991).

⁸L. J. Terminello and J. J. Barton, *Science* **251**, 1281 (1991).

⁹J. M. Plociennik, A. Barbet, and L. Mathey, *Surf. Sci.* **102**, 282 (1981).

¹⁰D. Aberdam, R. Baudoing, E. Blanc, and C. Gaubert, *Surf. Sci.* **71**, 279 (1978).

¹¹W. Mehlhorn, in *Atomic Inner Shell Physics*, edited by B. Crasemann (Plenum, New York, 1985).

¹²L. H. Jenkins and M. F. Chung, *Surf. Sci.* **28**, 409 (1971).

¹³C. M. K. Watts, *J. Phys. F* **2**, 574 (1972).

¹⁴H. Löfgren and L. Walldén, *Solid State Commun.* **12**, 19 (1973).

¹⁵J. C. Fuggle, *J. Phys. F* **7**, L81 (1977).

¹⁶J. Osterwalder (unpublished).

¹⁷G. Wiech, in *Soft X-ray Band Spectra*, edited by D. J. Fabian (Academic, London, 1968).

¹⁸R. Malutzki, A. Wachter, V. Schmidt, and J. E. Hansen, *J. Phys. B* **20**, 5411 (1987).

¹⁹S. Flüge, W. Mehlhorn, and V. Schmidt, *Phys. Rev. Lett.* **29**, 7 (1972).

²⁰J. Osterwalder, A. Stuck, D. J. Friedman, A. Kaduwela, C. S. Fadley, J. Mustre de Leon, and J. J. Rehr, *Phys. Scr.* **41**, 990 (1990).

²¹P. J. Feibelman, E. J. McGurie, and K. C. Pandey, *Phys. Rev. B* **15**, 2202 (1977).

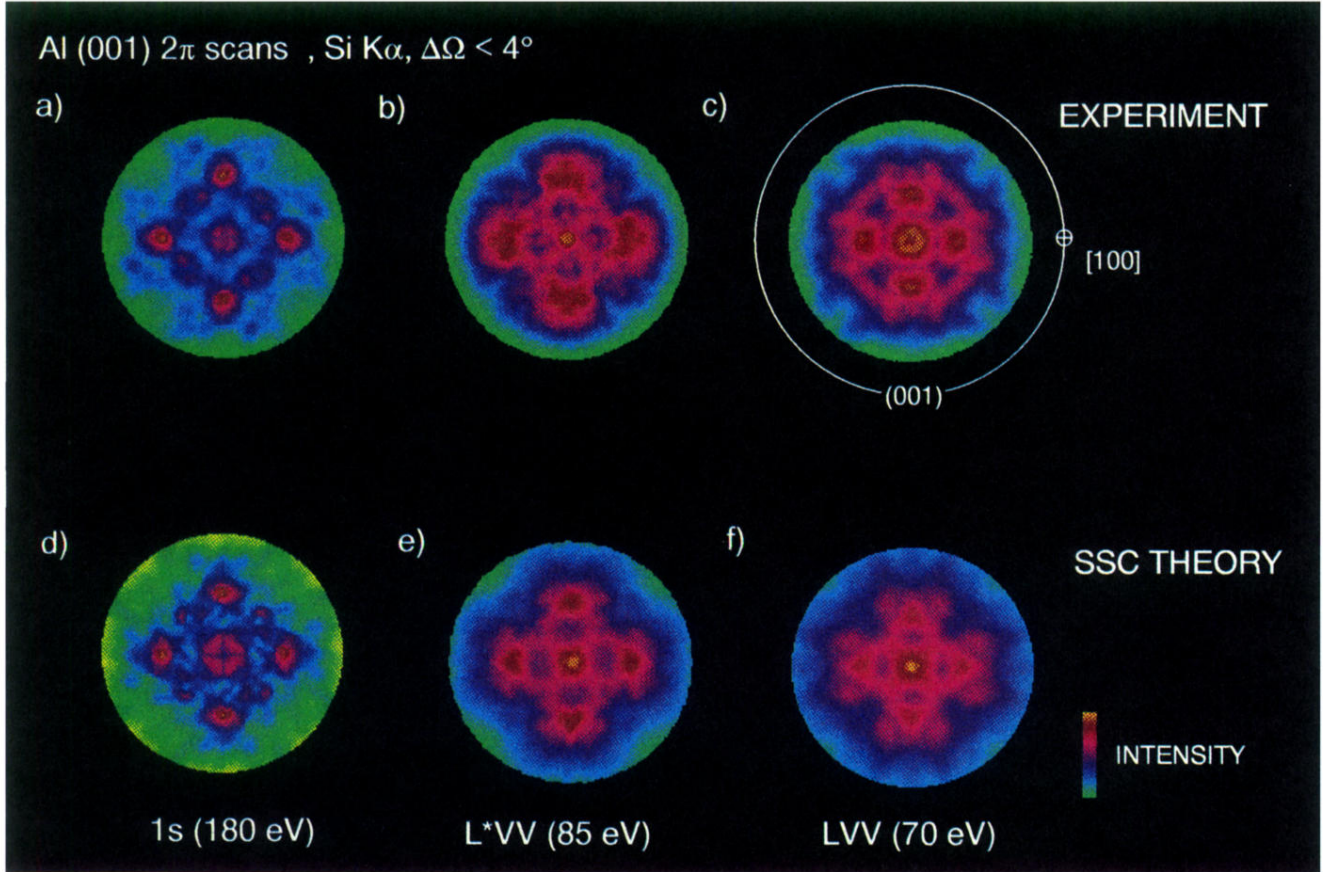


FIG. 3. Stereographically projected experimental and theoretical maps of electron emission intensities above an Al(001) surface. The intensities have been normalized with their maximum value in each plot. Each map consists of 3500 individually measured numbers. The experimental data [(a)–(c)] represent a total of 0.11, 0.22, and 0.21×10^9 counts for Al 1s (signal/background=0.27), L^*VV ($s/b=0.06$), and the LVV ($s/b=0.16$), respectively. The theory we applied to simulate these experiments considers single scattering only, and for the Al 1s emission p -wave final states aligned with the plane of polarization of our experiment. The L^*VV and LVV scans were simulated with incoherently added isotropic s , p , and d waves (see text).